

Adsorption of CO on Cu (110) and (100) surfaces using COSMO-based DFT

Zhijun Zuo · Wei Huang · Peide Han · Zhihong Li

Received: 19 December 2008 / Accepted: 18 January 2009 / Published online: 17 February 2009
© Springer-Verlag 2009

Abstract Density functional theory (DFT) combined with the conductor-like solvent model (COSMO) can provide valuable atomistic level insights into CO adsorption on Cu surface interactions in liquid paraffin. The objective of this research was to investigate the solvent effect of liquid paraffin. It was found that both structural parameters and relative energies are very sensitive to the COSMO solvent model. Solvent effects can improve the stability of CO adsorption on Cu (110) and (100) surfaces and the extent of CO activation.

Keywords Density functional theory · Carbon monoxide · Copper · Solvent effects · Adsorption

Introduction

Dimethyl ether (DME) has attracted much attention as an alternative diesel fuel due to its lower NO_x emissions and near-zero smoke, thus formation of DME from syngas (CO+H₂) conversion has recently generated increasing interest. There are two methods of “one-pot” synthesis of DME: the gas phase method, and the liquid phase method. The gas phase method generally uses a fixed bed reactor. The liquid phase

method uses a slurry reactor in which the catalyst is dispersed in a liquid medium such as liquid paraffin [1–5].

In “one-pot” synthesis of DME, the role of metallic copper in the reaction mechanism has been discussed widely in the literature over the past 20 years and remains a matter of debate. Today, it is widely accepted that the final active catalyst is obtained by reduction of CuO to metallic Cu under a diluted H₂ flow before feeding the synthesis gas mixture [1, 6–7]. Because of the importance of adsorption, the interaction of CO molecules with Cu (111), (110) and (100) surfaces under vacuum has been studied by many researchers [8–11]. To the best of our knowledge, despite intense experimental activity, a detailed understanding of the general rules governing the interaction of CO with Cu surfaces in liquid paraffin is still lacking. XRD characterization has proved that Cu (111), (100) and (110) are the main surfaces of the copper [12, 13]. In order to study differences in the adsorption of CO molecules on Cu surfaces in vacuum and in liquid paraffin, adsorption of CO molecules on Cu surfaces is studied. Although the intensity of the Cu(111) peak is higher than that of the other peaks, it is known that the lower peak always shows higher activity [14]. Thus, in this article, the adsorption behavior of CO molecules adsorbed onto Cu (100) and (110) surfaces is studied. The results may be of interest to researchers attempting to investigate the specific aspects of the syngas (CO+H₂) conversion such as the DME synthesis reaction.

Calculated models and details

The general principles of the DFT-pseudopotential method have been described elsewhere [15–17]. The generalized gradient corrected exchange-correlation functional pro-

Z. Zuo · W. Huang (✉) · Z. Li
Key Laboratory of Coal Science and Technology
of Ministry of Education and Shanxi Province,
Taiyuan University of Technology,
Taiyuan, Shanxi 030024, China
e-mail: huangwei@tyut.edu.cn

P. Han
College of Materials Science and Engineering,
Taiyuan University of Technology,
Taiyuan, Shanxi 030024, China

posed by Perdew and Wand (PW91) [18] was chosen together with the doubled numerical basis set plus polarization basis sets (DND, including the polarization d-function) [19]. The electronic structures were obtained by solving the Kohn-Sham (KS) [20, 21] equation self-consistently in the condition of spin unrestricted while the all-electron relativistic DFT is used for core electrons. A self-consistent field (SCF) procedure was carried out with a convergence criterion of 10^{-5} a.u. on energy and electron density, and geometry was optimized under a symmetry constraint with the convergence criteria of 10^{-3} a.u. on the gradient and 10^{-3} a.u. on the displacement.

The equilibrium lattice constants of Cu are $a_{\text{Cu}} = 3.685$ Å, while an experimental value of $a_{\text{Cu}} = 3.615$ Å was found, i.e., there was good agreement between our computed value and the experimental datum reported by Kittel [22]; the discrepancy is less than 2%. The substrates are modeled by four layers of metal separated by a vacuum region 10 Å wide. The three uppermost substrate layers and the CO molecule are allowed to relax, keeping the volume constant. A $p(2 \times 2)$ cell is used for the Cu (110) and (100) surfaces.

We have also applied COSMO (conductor screening model [23, 24]) to simulate the dielectric response of the environment. COSMO is a continuum solvent model where the solute molecules form a cavity within the dielectric continuum of permittivity ϵ that represents the solvent. The charge distribution of the solute polarizes the dielectric medium. The response of the dielectric medium is described by the generation of screening (or polarization) charges on the cavity surface. In contrast to other implementations of continuum solvent models, COSMO does not require solution of the rather complicated boundary conditions for a dielectric in order to obtain screening charges, but instead calculates the screening charges using a much simpler boundary condition for a conductor. These charges are then scaled by a factor $f(\epsilon) = (\epsilon - 1) / (\epsilon + 0.5)$, to obtain a rather good approximation of the screening charges in a dielectric medium. The deviations of this COSMO approximation from the exact solution are rather small.

For strong dielectrics like water they are less than 1%, while for nonpolar solvents with $\epsilon \approx 2$ they may reach 10% of the total screening effects. However, for weak dielectrics, screening effects are small, and the absolute error therefore amounts to less than 1 kcal mol $^{-1}$. The model provides accurate calculation of gradients, which allows geometry optimization of the solute within the dielectric continuum. The dielectric constant of liquid paraffin is considered as $\epsilon = 2.06$. COSMO cannot be used under vacuum conditions.

Results and discussion

To investigate the reliability of the calculation, we calculated the bond length and vibrational stretching frequencies of free CO, which are 1.141 Å and 2,116.1 cm $^{-1}$, respectively. There is thus good agreement between our calculation and the experimental values of 1.128 Å and 2,170 cm $^{-1}$, respectively [25].

It is well known that the adsorption energy of C-down is more favorable than that of O-down on the same adsorption site according to the experimental and calculated results, so we calculate only C adsorbing to the Cu surface [26]. The chemisorption energy per CO molecule is defined as $E_{\text{ads}} = E(\text{CO/slab}) - [E(\text{CO}) + E(\text{slab})]$ [27], where the first term is the total energy for the slab with the chemisorbed CO on the surface, the second term is the total energy of free CO, and the third term is the total energy of the bare slab of the surface. Therefore, a negative E_{ads} value means exothermic chemisorption, and a positive E_{ads} value means endothermic chemisorption.

CO chemisorption on Cu (110)

Our calculation begins with 1/4 ML coverage of Cu (110)– (2×2) , and the k point of $3 \times 5 \times 2$ Monkhorst-Pack meshes was used. According to the surface morphology, there are three different adsorptive sites (Fig. 1)—top, short bridge and long bridge—and three possible surface structures are obtained. Adsorption energies and struc-

Fig. 1 Structures of chemisorbed CO on Cu (110). Adsorption sites: *T* Top site, *LB* long bridge, *SB* short bridge

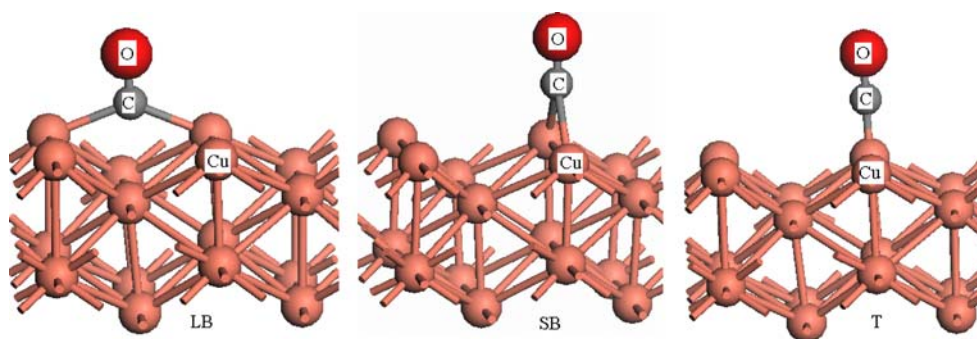


Table 1 Computed chemisorption energies (E_{ads} , eV) per molecule, CO and C–Cu bond length (Å) and Mulliken charges of C and O as well as net charges of CO at different sites on Cu (111) for a coverage of 1/4 ML: E_{ads} Adsorption energy; $d_{\text{C-O}}$ carbon-oxygen bond length; $d_{\text{Cu-C}}$ copper-carbon bond length; q_{C} , q_{O} Mulliken charges of C and O, respectively, q_{CO} net charge of CO^a

110	Vacuum			Liquid paraffin			Free CO
	T ^b	SB	LB	T	SB	LB	
E_{ads}	-1.09	-1.13	-0.66	-1.63	-1.78	-1.09	
$d_{\text{Cu-C}}$	1.831	1.985	2.068	1.957	1.962	2.000	
$d_{\text{C-O}}$	1.155	1.168	1.186	1.185	1.186	1.210	1.141
q_{C}	0.369	0.346	0.308	0.333	0.311	0.321	0.105
q_{O}	-0.135	-0.148	-0.175	-0.221	-0.226	-0.273	-0.105
q_{CO}	0.234	0.198	0.133	0.112	0.085	0.048	0

^a Net charges of CO, $q_{\text{CO}} = q_{\text{C}} + q_{\text{O}}$

^b Adsorption sites: *T* Top site, *LB* long bridge, *SB* short bridge

tural parameters are listed in Table 1. All three structures have exothermic chemisorption energies, indicating that CO chemisorption on Cu (110) is thermodynamically favored. The most stable chemisorbed structure (short bridge) has an adsorption energy of -1.13 eV, while the top and the long bridge are less stable (-1.09 and -0.66 eV, respectively). The chemisorption energies decrease about 0.5 eV–0.7 eV of all the adsorption models influenced by solvent effects. The result shows that the liquid paraffin solvent can improve the adsorptive ability. However, no experimental data are available for comparison with our calculated chemisorption energies.

As Cu (110) surface adsorbs CO, in the top (one-fold site), CO interacts with one adjacent Cu atom and forms one Cu–C bond in vacuum, and the C–O bond is elongated compared to free CO (1.155 Å vs 1.141 Å). In the short bridge (2-fold bridge site), CO interacts with two adjacent Cu atoms and forms two Cu–C bonds, and the C–O bond is

Table 2 Computed chemisorption energies (E_{ads} , eV) per molecule, CO and C–Cu bond length (Å) and Mulliken charges of C and O as well as net charges of CO at different sites on Cu (111) for a coverage of 1/4 ML

100	Vacuum			Liquid paraffin		
	T ^a	B	H	T	B	H
E_{ads}	-0.90	-0.86	-0.80	-1.08	-1.06	-0.99
$d_{\text{Cu-C}}$	1.854	1.986	2.157	1.855	2.009	2.253
$d_{\text{C-O}}$	1.153	1.169	1.195	1.164	1.184	1.197
q_{C}	0.354	0.347	0.266	0.307	0.286	0.270
q_{O}	-0.124	-0.142	-0.174	-0.174	-0.211	-0.229
q_{CO}	0.23	0.205	0.092	0.133	0.075	0.041

^a Adsorption sites: *T* Top site, *H* hollow site, *B* bridge site

elongated to 1.168 Å. In the long bridge, CO also interacts with two Cu atoms on the surface, and the C–O bond is elongated to 1.186 Å.

As the Cu surface adsorbs CO in liquid paraffin, all the C–O and Cu–C bonds of the three adsorption models are longer than the corresponding adsorption models in vacuum. The result shows the liquid paraffin solvent not only reduces the chemisorption energies but also influences the C–O and Cu–C bonds. According to the monitor bonding function of the dmol³, nondissociative adsorption when the Cu surface is adsorbed by CO either in vacuum or liquid paraffin.

CO chemisorption on Cu (100)

The *k* point of 5×5×2 Monkhorst-Pack meshes is used. According to the Cu (100) surface morphology, there are also three different adsorptive sites (in Fig. 2): top, bridge and hollow. Adsorption energies and structural parameters are listed in Table 2.

Fig. 2 Structures of chemisorbed CO on Cu (100). Adsorption sites: *T* Top site, *H* hollow site, *B* bridge site

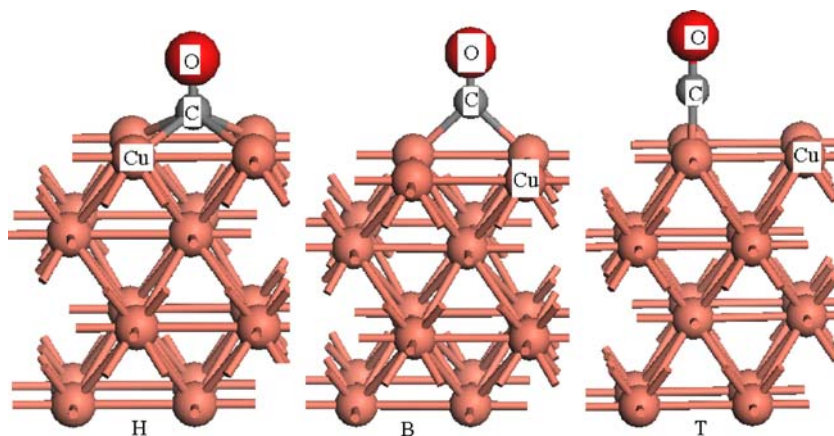


Figure 2 shows three different adsorptive models. In vacuum, CO interacts with one Cu atom and forms one Cu–C in the top site, and the C–O bond is elongated compared to free CO (1.153 Å vs 1.141 Å). In bridge (2-fold bridge site), CO interacts with two adjacent Cu atoms and forms two Cu–C bonds, and the C–O bond is elongated to 1.169 Å. In the hollow site (4-fold site), CO interacts with four Cu atoms and the C–O bond is elongated to 1.195 Å. The Cu–C distance varies in the interval from 1.854 to 2.157 Å, and increases with coordination.

As the Cu surface adsorbs CO in liquid paraffin, all the C–O and Cu–C bonds of three adsorption models are longer than the corresponding adsorption models in vacuum. According to the monitor bonding function of the dmol^3 , they are both nondissociative adsorption when the Cu surface is adsorbed by CO in vacuum or liquid paraffin, which is in agreement with the experiment results of HREELS, LEED, TPD and so on [28–30].

As given in Table 2, all three structures have exothermic chemisorption energies, indicating that CO chemisorption on Cu (100) is thermodynamically favored. The greater the exothermic chemisorption energies, the more stable the adsorption models, so the thermodynamic preference of CO nondissociative chemisorption shows the order $E_{\text{ads}}(\text{top}) > E_{\text{ads}}(\text{bridge}) > E_{\text{ads}}(\text{hollow})$ in vacuum. The result agrees well with both experiment and theory, in which the CO adsorbs the Cu surface with top mode [10, 31]. The chemisorption energies decrease by about 0.2 eV of all the adsorption models influenced by solvent effects. The result shows that liquid paraffin solvent can promote the stability of CO adsorption on the Cu (100) surface.

As shown in Tables 1 and 2, the C–O bond increases with the number of Cu atoms to which the molecule binds in both environments. It is well known that there are two kinds of interaction between the metal and other molecules [32, 33]. One is the interaction between the adsorbates, another is the interaction between the metal and the adsorbates. There is no significant repulsion between chemisorbed CO molecules at 1 ML [32], so the adsorptive structure is influenced mainly by the direct interaction of CO and Cu. In other words, the bonds change trend in different models, showing that the C–O bonds are effected mainly by Cu and CO interaction. The net charge of the chemisorbed CO on the Cu (110) and (100) surface given in Tables 1 and 2 can be compared with those of free CO. This shows clearly that the chemisorbed CO molecules are partially positively charged, indicating electron transfer from CO into the copper surface. The elongation of the C–O bonds increases with the decrease in the net charges of chemisorbed CO molecules. It indicates that stronger electron transfer from the surface into the antibonding orbital of CO induces higher activation of the C–O bonds. When CO molecules are adsorbed on the Cu (hkl) surface,

the C–O bonds in liquid paraffin are longer than bonds of C and O in vacuum. This indicates that CO molecules induce higher activation of C–O bonds in liquid paraffin than in vacuum.

Combined with the chemisorption energy of CO adsorption on Cu (111) (Z. Zuo et al., manuscript submitted), the ability of CO chemisorption on the copper surfaces is in the order $\text{Cu (110)}(-1.13 \text{ eV}) > \text{Cu (111)}(-0.98 \text{ eV}) > \text{Cu (100)}(-0.90 \text{ eV})$ in vacuum; however, the thermodynamic preference of CO nondissociative chemisorption shows the order $\text{Cu (110)}(-1.78 \text{ eV}) > \text{Cu (111)}(-1.09 \text{ eV}) \approx \text{Cu (100)}(-1.09 \text{ eV})$ in liquid paraffin.

Conclusions

Chemisorption of CO on Cu (100) and Cu (110) surfaces was investigated using the generalized gradient approximation (GGA) and the Perdew and Wang (PW91) functional at the level of DFT. On both surfaces, CO is chemisorbed by nondissociative adsorption, and has elongated C–O bond lengths. The C–O bonds in liquid paraffin are longer than the C–O bonds in vacuum, thus solvent effects can improve CO activation.

On the basis of the computed chemisorption energies, CO chemisorption is exothermic on Cu (110) and Cu (100) surfaces; however, the stability of chemisorption of CO on the Cu (110) is larger than on the Cu (100) surface. Owing to the solvent effect, the stability of CO adsorption on the Cu (100) and Cu (110) surfaces increases. Meanwhile, the change in the nondissociative chemisorption energies of the Cu (110) surface are larger than those of the Cu (100) surface. These results might mean that syngas ($\text{CO} + \text{H}_2$) conversions such as the DME synthesis reaction could be improved in a slurry reactor.

Acknowledgment The authors gratefully acknowledge the financial support of this study by the National Natural Science Foundation of China (Grant No.20676087), the National Basic Research Program of China (Grant No 2005CB221204).

References

1. Figueiredo RT, Martinez-Arias A, Granados ML, Fierro JLG (1998) *J Catal* 178:146–152
2. Marbán G, Fuertes AB (2005) *Appl Catal B* 57:43–53
3. El-Shobaky GA, Ghosza AM (2004) *Mater Lett* 58:699–705
4. Brookhaven National Laboratory, (1986) US Patent, 461479, 4619946, 4623634, 4613623, 4935395 (1990)
5. Yang RQ, Yu XC, Zhang Y, Li WZ, Tsubaki N (2008) *Fuel* 87:443–450
6. Chinchén GC, Mansfield K, Spencer MS (November 1990) *Chem Tech* 692–699
7. Herman RG (1991) *Stud Surf Sci Catal* 27:265–349

8. Wang GC, Jiang L, Pang XY, Cai ZS, Pan YM, Zhao XZ, Morikawa Y, Nakamura J (2003) *Surf Sci* 543:118–130
9. Ge Q, King DA (2001) *J Chem Phys* 114:1053–1054
10. Graham AP, Toennies JP (2001) *J Chem Phys* 114:1051–1052
11. Neef M, Doll K (2006) *Surf Sci* 600:1085–1092
12. Gao ZH, Hao LF, Huang W (2005) *Catal Lett* 102:139–141
13. Gao ZH, Huang W, Yin LH, Hao LF, Xie KC (2009) *Catal Lett* 127:354–359, doi:10.1007/s10562-008-9689-9
14. Raybaud P, Digne M, Ifimie R, Wellens W, Euzen P, Toulhoat H (2001) *J Catal* 201:236–246
15. Ordejón P, Artacho E, Soler JM (1996) *Phys Rev B* 53: R10441–R10444
16. Grochala W (2008) *J Mol Model* 14:887–890
17. Artacho E, Sánchez-Portal D, Ordejón P, García A, Soler JM (1999) *Phys Status Solidi B* 215:809–817
18. Dolg M, Liu W, Kalvoda S (2000) *Int Quantum Chem* 76:359–370
19. Hirshfeld FL (1977) *Theor Chim Acta* 44:129–138
20. Yun L, Florent B, Chafika G, Zhang Y, Maurel F, Hu Y, Fan BT (2008) *J Mol Model* 14:901–910
21. Kohn W, Sham LJ (1965) *Phys Rev A* 140:1133–1137
22. Charles K (1976) *Introduction to solid state physics*, 5th edn. Wiley, New York, p 23
23. Tajkhorshid E, Suhai S (2000) *J Mol Struct (THEOCHEM)* 501–502:297–313
24. Klamt A, Schürmann GJ (1993) *Chem Soc Perkin Trans* 25:799–805
25. Lide DR (1992) *CRC handbook of chemistry and physics*, 73th edn. CRC, Florida
26. Blyholder G (1964) *J Phys Chem* 68:2772–2778
27. Wang SG, Cao DB, Li YW, Wang JG, Jiao HJ (2005) *J Phys Chem B* 109:18956–18963
28. Tracy JC (1964) *J Chem Phys* 68:2772–2778
29. Truong CM, Rodriguez JA, Goodman DW (1992) *Surf Sci* 271: L385–L391
30. Yeo YY, Vattuone L, King DA (1996) *J Chem Phys* 104:3810–3821
31. Gajdoš M, Hafner J (2005) *Surf Sci* 590:117–126
32. Kresse G, Gil A, Sautet P (2003) *Phys Rev B* 68:073401–073401
33. Zhao XX, Mi YM (2008) *Acta Phys-Chim Sin* 24:127–131